Defect and Diffusion Forum Vol. 336 (2013) pp 169-184
Online available since 2013/Mar/25 at www.scientific.net

doi:10.4028/www.scientific.net/DDF.336.169

Phonon Thermal Conductivity of f.c.c. Cu by Molecular Dynamics Simulation

Leila Momenzadeh[1], Alexander V. Evteev[1,a], Elena V. Levchenko[1], Irina V. Belova[1] and Graeme E. Murch[1], Yongho Sohn[2]

[1]The University Centre for Mass and Thermal Transport in Engineering Materials
Priority Research Centre for Geotechnical and Materials Modelling
School of Engineering The University of Newcastle
Callaghan, NSW 2308, Australia

[2]Department of Materials Science and Engineering University of Central Florida
4000 Central Florida Blvd. Orlando, FL 32816-2455, USA

[a]alexander.evteev@newcastle.edu.au

Keywords: thermal conductivity, phonons, molecular dynamics, Green-Kubo method, copper.

Abstract. Phonon dynamics and phonon thermal conductivity of f.c.c. Cu are investigated in detail in the temperature range 200 – 1300 K within the framework of equilibrium molecular dynamics simulations making use of the Green-Kubo formalism and one of the most reliable embedded-atom method potentials. It is found that the temporal decay of the heat current autocorrelation function of the f.c.c. Cu model at low and intermediate temperatures demonstrates a more complex behaviour than the two-stage decay observed previously for the f.c.c. Ar model. After the first stage of decay, it demonstrates a peak in the temperature range 200 – 800 K. The intensity of the peak decreases as the temperature increases. At 900 K, it transforms to a shoulder which diminishes almost entirely at 1200 K. It is suggested that the peak may be activated by the influence of the Cauchy pressure in f.c.c. Cu on the phonon dynamics. A decomposition model of the heat current autocorrelation function of a monatomic f.c.c. lattice is introduced. This model can capture all contributions to the function discussed in the literature. It is found that the temperature dependence of the phonon thermal conductivity of the f.c.c. Cu model is in good agreement with previous calculations on the f.c.c. Ar model which follows an exponent close to -1.4, i.e. varies more rapidly than the T^{-1} law predicted by the theory. The calculated phonon thermal conductivity of the f.c.c. Cu is found to be about one order of magnitude higher than the f.c.c. Ar. This is explained by the inclusion of the electronic contribution to the bulk lattice properties during the fitting of the embedded-atom method potential functions to the experimental or *ab initio* data. It is demonstrated that the electronic contribution to the total thermal conductivity of f.c.c. Cu dominates over the whole studied temperature range. Nevertheless, the phonon contribution increases as the temperature decreases. The contribution can be estimated to be about 0.5 % at 1300 K and about 5 % at 200 K.

Introduction

It is well known that during phase transformations or recrystallization processes, latent heat gives rise to a thermal gradient in the local region surrounding an interface. As a result, the interface mobility, which is one of the most important properties of an interface, can be affected [1]. Despite the importance of interface mobility in understanding the physics underlying the kinetics of phase transformation or recrystallization, there are only a few successful experimental measurements of interface mobility [2,3]. Currently, much of our understanding of kinetics properties of interfaces has been derived from molecular dynamics (MD) simulations [1,4,5]. However, one would expect that classical MD simulations of metals underestimate the magnitude of thermal conductivity due to absence of the free-electron contribution [6]. Accordingly, without an accurate knowledge of thermal conductivity it is difficult to assess how classical MD simulations of metals such as

employing embedded-atom method (EAM) interatomic potentials [7] are able to come close to predicting the kinetics properties of interfaces. Indeed, there is a concern in predicting nonequilibrium flows in the local region surrounding an interface, since the free-electron contribution to the thermal conductivity can outweigh the phonon contribution [6].

In an early study [6] nonequilibrium MD simulations with an EAM potential [8] were used to estimate phonon thermal conductivities of f.c.c Cu and Au under large temperature gradients. In particular, this relatively crude method allowed the authors to estimate an average (over a wide temperature range) thermal conductivity of the MD model of Cu with EAM potential [8] of about 5.7 W/mK. This is a factor of 68 smaller than the experimental value of 385 W/mK at 500 K [9]. However, the average thermal conductivity of the MD model of Cu is considerably higher than that of an insulating material. For example, the thermal conductivity is one order of magnitude higher that of a Lennard-Jones pair potential model for f.c.c. Ar [10]. A larger value of phonon thermal conductivity predicted by an EAM potential model compared with a pair potential model can be explained by the inclusion of the electronic contribution to the bulk lattice properties during the fitting of the EAM potential functions to the experimental or *ab initio* data. As a result, in particular, an EAM potential model, in contrast to a pair potential model, is able to describe the positive (non-zero) Cauchy discrepancy (Cauchy pressure) C_{12}-C_{44} (where C_{12} and C_{44} are the elastic constants) which is one of the generic features of bulk lattice properties of real metals [7].

Another approach to calculate the thermal conductivity by using MD simulations is to employ the Green-Kubo (GK) formalism [11,12]. The GK method is based on an equilibrium system and for an isotropic material gives the thermal conductivity, k, as the time integral of the heat current autocorrelation function (HCACF), $\langle \boldsymbol{J}(t)\boldsymbol{J}(0)\rangle$, [13]:

$$k = \frac{1}{3Vk_{\mathrm{B}}T^2}\int_0^{\infty}\langle \boldsymbol{J}(t)\boldsymbol{J}(0)\rangle dt, \tag{1}$$

where V is the volume of the simulation cell, k_{B} is the Boltzmann, T is temperature, $\boldsymbol{J}$ is the heat current and t is time. The heat current can be defined [10] as:

$$\boldsymbol{J} = \frac{d}{dt}\left(\sum_i E_i \boldsymbol{r}_i\right) = \sum_i E_i \boldsymbol{v}_i + \sum_i \boldsymbol{r}_i \frac{dE_i}{dt}, \tag{2}$$

where the summation is over the atoms in the system, and E_i is the energy (kinetic and potential) of the i-th atom, $\boldsymbol{r}_i$ is the radius-vector of the i-th atom and $\boldsymbol{v}_i$ is the velocity vector of the i-th atom. Implementation of the GK method has no effect on the atomic dynamics and the system temperature is uniform and constant. In addition, this method allows for calculation of the temperature dependence of the thermal conductivity. Furthermore, one can use the equilibrium MD simulations to investigate phonon dynamics, for example, by analysing HCACF [10].

In the last decade, the GK method has been successfully used to calculate the thermal conductivity of f.c.c. Ar [10,14,15]. Crystal argon is a natural choice for a benchmark study of lattice thermal conductivity. First, the interatomic forces in this system are known to be adequately described by the Lennard-Jones pair potential [9]. Second, experimental data [16,17] are available for validating the accuracy of the simulation results. Below, we briefly summarize the main results of these calculations.

In contrast to the Peierls theory of thermal conductivity [18], which is consistent with a single-stage decay of the HCACF [10,14,15,19], the authors [10,14] observed the two-stage decay in the HCACF of f.c.c. Ar. It should be noted that the two-stage decay in the HCACF was first observed in MD simulations [19]. Based on the observed shape of the HCACF of f.c.c. Ar, McGaugey and Kaviany [10,14] fitted this function to a sum of two exponential functions as suggested by Che *et al.* [20]:

$$\frac{1}{3}\langle \boldsymbol{J}(t)\boldsymbol{J}(0)\rangle = A_{\mathrm{ac,sh}}\exp\left(-t/\tau_{\mathrm{ac,sh}}\right) + A_{\mathrm{ac,lg}}\exp\left(-t/\tau_{\mathrm{ac,lg}}\right), \tag{3}$$

where $\tau_{\mathrm{ac,sh}}$ and $\tau_{\mathrm{ac,lg}}$ are the time constants, and $A_{\mathrm{ac,sh}}$ and $A_{\mathrm{ac,lg}}$ are the strengths. The first and second terms in Eq. (3) describe two time scales of the decay, which are associated with short and long wavelength acoustic phonons, respectively (optical phonons cannot be present, as the unit cell is monatomic). The first time scale in the HCACF decomposition according to [10,14] is related to how long it takes for energy to move between nearest-neighbour atoms. The associated phonons have mean free paths equal to one half of their wavelength. This smallest physically meaningful value corresponds to the lower bound on the phonon mean free path, known as the Cahill and Pohl limit [10,14,21,22]. In this case, one can visualize the movement of a phonon through a system as a series of energy transfers between neighbouring atoms [10, 14]. Thus, the first term in Eq. (3) should be strongly a function of the coordination of the atoms [10,14]. The second time scale is longer, and corresponds to acoustic phonons with mean free paths longer than one half of their wavelength [10,14]. With Eqs. (1) and (3), the thermal conductivity is then given by:

$$k = \frac{1}{Vk_{\mathrm{B}}T^2}\left(A_{\mathrm{ac,sh}}\tau_{\mathrm{ac,sh}} + A_{\mathrm{ac,lg}}\tau_{\mathrm{ac,lg}}\right) = k_{\mathrm{ac,sh}} + k_{\mathrm{ac,lg}}. \quad (4)$$

McGaugey and Kaviany [10,14] pointed out that in the decomposition given by Eq. (4), all of the temperature dependence of the thermal conductivity is contained in $k_{\mathrm{ac,lg}}$, while the short-range component, $k_{\mathrm{ac,sh}}$, shows little temperature dependence. This behaviour is a result of the coordination of the atoms remaining constant as the density changes with temperature. Overall, the predicted temperature dependence of thermal conductivity of the MD model of the f.c.c Ar was found to be in agreement with the trend and magnitude of experimental data.

Using the Lennard-Jones pair potential with a longer cutoff radius, Kaburaki *et al.* [15] also demonstrated that the temperature dependence of the experimentally measured thermal conductivity of f.c.c Ar can be reproduced with good accuracy by the equilibrium MD simulation in conjunction with the GK method. In addition, the authors [15] found that the absolute values of the thermal conductivity and the two-stage relaxation of the HCACF are in agreement with the results reported by McGaugey and Kaviany [10,14]. However, Kaburaki *et al.* [15] differ from the previous authors [10,14] in the interpretation and analysis of the HCACF. They attribute the first-stage of relaxation to single-particle motions sampling the local environment of the system, whereas McGaugey and Kaviany [10,14] regard this relaxation to be associated with short wavelength acoustic phonons as we mentioned above. Furthermore, Kaburaki *et al.* [15] pointed out that the first stage of relaxation is not properly described by a single exponential function. Indeed, they observed a slight shoulder at short times at low and intermediate temperatures, which had not been noted previously. The authors [15] suggested that it may be associated with collective oscillations, possibly of a transverse or shear nature and highly damped. Nonetheless, Kaburaki *et al.* [15] also expect that overall the first stage of relaxation of the HCACF to be relatively insensitive to temperature, because the local environment surrounding a particle does not change much even when the system goes from a low-temperature solid to the liquid phase and loses long-range ordering. Regarding the second stage of relaxation of the HCACF, Kaburaki *et al.* [15] are in agreement with McGaugey and Kaviany [10,14] that the underlying process is lattice vibrations or phonons. According to [15], this part is also expected to be sensitive to temperature variations because long-range ordering is needed to sustain the collective motions.

Thus, the commonly accepted main feature of the HCACF of f.c.c. Ar predicted by the equilibrium MD simulation with Lennard-Jones pair potential is a two-stage decay (relaxation) [10,14,15]. This is in contrast to the Peierls theory of thermal conductivity [18], which is consistent with a single-stage decay of the HCACF [10,14,15,19]. Unfortunately, we could not find in the literature any results on phonon thermal conductivity calculations in metals within the framework of the EAM method using the equilibrium MD simulations in conjunction with the GK formalism. However, besides the abovementioned importance of knowledge of the phonon thermal conductivity in problems dealing with predicting the kinetics properties of interfaces in metals by classical MD simulations, the fundamental interest would also be to investigate phonon dynamics in

an EAM potential model by analysing its HCACF in comparison with the HCACF of the Lennard-Jones pair potential model of argon. One of the appropriate candidates for these studies is copper: (i) Cu, like Ar, has the f.c.c. lattice that makes comparison of results convenient; (ii) a very high-quality EAM potential [23] is available for Cu; (iii) the calculated phonon thermal conductivity can be compared to the previous nonequilibrium MD calculations [6] of the phonon thermal conductivity of f.c.c Cu under a large temperature gradient with older EAM potential [8].

Therefore, the purpose of this paper is to investigate in detail the temperature dependencies of the phonon thermal conductivity and phonon dynamics of f.c.c. Cu by analysing HCACF extracted from the equilibrium MD simulations at different temperatures and zero pressure, using one of the most reliable EAM potentials known up to now. In addition, our objective is to compare the results obtained to those that for the Lennard-Jones pair potential model of f.c.c. Ar [10,14,15].

Calculation methods

In this work, the interactions between atoms in the MD model of f.c.c. Cu are described by using an EAM potential developed by Mishin *et al.* [23]. The potential was obtained by fitting to experimental and first-principles data. This potential accurately reproduces the lattice parameter, cohesive energy, elastic constants, phonon frequencies, thermal expansion, lattice-defect energies, and other relevant properties of Cu. The melting temperature of Cu predicted by this potential is 1327 K in good agreement with the experimental value of 1357 K [24].

In the present calculations, we considered the temperature range 200 – 1300 K with a temperature step 100 K. It was previously argued [10,20] that the dominant contributions to the thermal transport are long wavelength phonons active even at low temperature and, consequently, there is no evidence to support the use of quantum corrections with the classical MD thermal conductivity predictions at relatively low temperatures, up to around one-tenth of the Debye temperature [10]. Despite this, in the present study, we decided not to go far below the Debye temperature of Cu which is 343 K [25]. This is in contrast to the specific heat, where it is the high-frequency (short wavelength) modes that become excited as the temperature of the quantum system is increased and lead to the significant temperature dependence up to the Debye temperature [10].

All reported data are averaged over the MD simulations in the *NPT* (isothermal-isobaric), *NVT* (canonical) and *NVE* (microcanonical) ensembles at zero pressure. The cubic simulation block was composed of 4,000 atoms with periodic boundary conditions in all three directions. We started our MD simulations in the *NPT* ensemble. Then, the obtained equilibrium (zero pressure) value of the system volume at each temperature was used as an input for the MD simulations in the *NVT* and *NVE* ensembles. The obtained temperature dependence of the equilibrium (zero pressure) atomic volume of the f.c.c. Cu model is shown in Fig. 1. It is in good agreement with the linear thermal expansion data for the EAM model of Cu published in [23]. The atomic volume versus temperature curve can be nicely fitted by the equation:

$$\Omega = \Omega_0 + \alpha_\Omega T + \beta_\Omega T^2 \tag{5}$$

with $\Omega_0 \approx 11.82\times10^{-3}$ nm^3/atom, $\alpha_\Omega \approx 4.5\times10^{-7}$ nm^{3}K^{-1}/atom and $\beta_\Omega \approx 1.8\times10^{-10}$ nm^{3}K^{-2}/atom. After equilibration of the system at a given temperature by performing a run of $10^5\Delta t$ (Δt=1.5fs is the time step), the HCACF was calculated during a production run of additional $10^6\Delta t$ (for 200 K and 300 K the production runs were even longer, see below). It should be noted that in order to set a given temperature for the *NVE* ensemble, the first $5\times10^4\Delta t$ of the equilibration run was always done in the *NVT* ensemble. A correlation length of $10^4\Delta t$ with about 10^5 time origins was used to calculate the HCACF in the temperature range 400 – 1300 K. At lower temperatures, the correlation time is longer. Hence, to calculate the HCACF, correlation lengths of $5\times10^4\Delta t$ with about 10^6 time origins and $2\times10^4\Delta t$ with about 2×10^5 time origins in the production runs of $10^7\Delta t$ and $2\times10^6\Delta t$ were used at 200 K and 300 K, respectively.

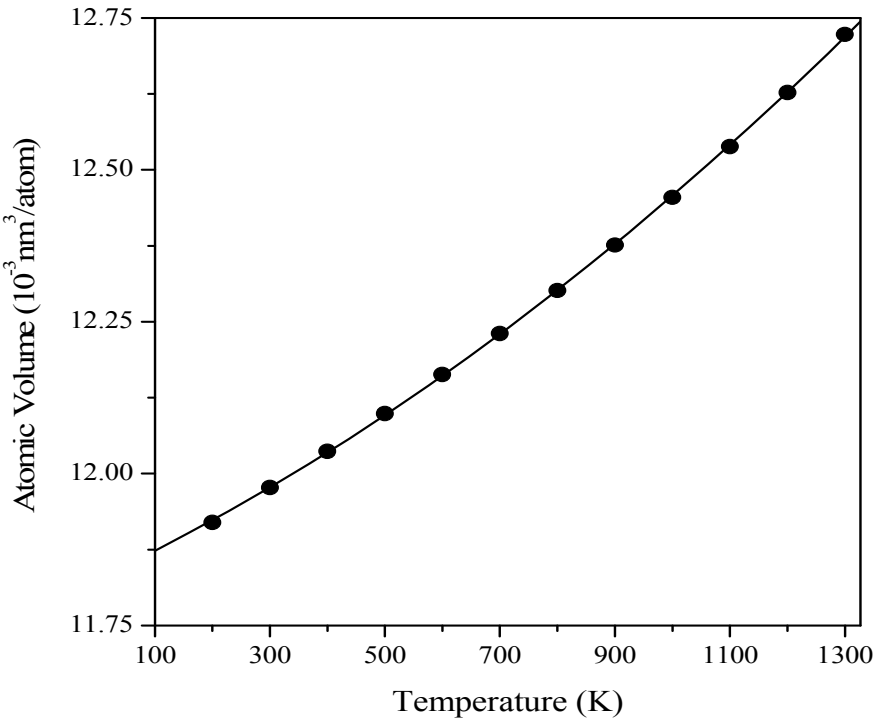

Fig. 1. Temperature dependence of the equilibrium atomic volume of the EAM potential model [23] of f.c.c. Cu according to MD simulations in the *NPT* ensemble. The solid line shows the fit of the MD data by Eq. (5).

As a sensitivity test of system size, calculations were performed with the cubic simulation block composed of 32,000 atoms at a temperature of 500 K. We found very good agreement between the HCACFs and thermal conductivities predicted from simulation blocks containing 4,000 and 32,000 atoms. Also, as a sensitivity test of the length of the production run, calculations were performed with the simulation block composed of 4,000 atoms at temperatures of 500, 700 and 1300 K using a correlation length of $5\times10^4\Delta t$ with about 10^6 time origins in the production run of $10^7\Delta t$. Again, very good agreement with our previous simulations was found.

Results and discussion

In Fig. 2, we show, as an example, the HCACF calculated at 200, 400, 600, 800, 1000 and 1200 K for *NPT*, *NVT* and *NVE* ensembles as well as the averaged over the three ensembles. The HCACF is normalized by its zero time value to allow for comparison between the different temperatures. It can be seen that the four curves sit very close to each other at a given temperature. This fact is reassuring for calculations in all three ensembles.

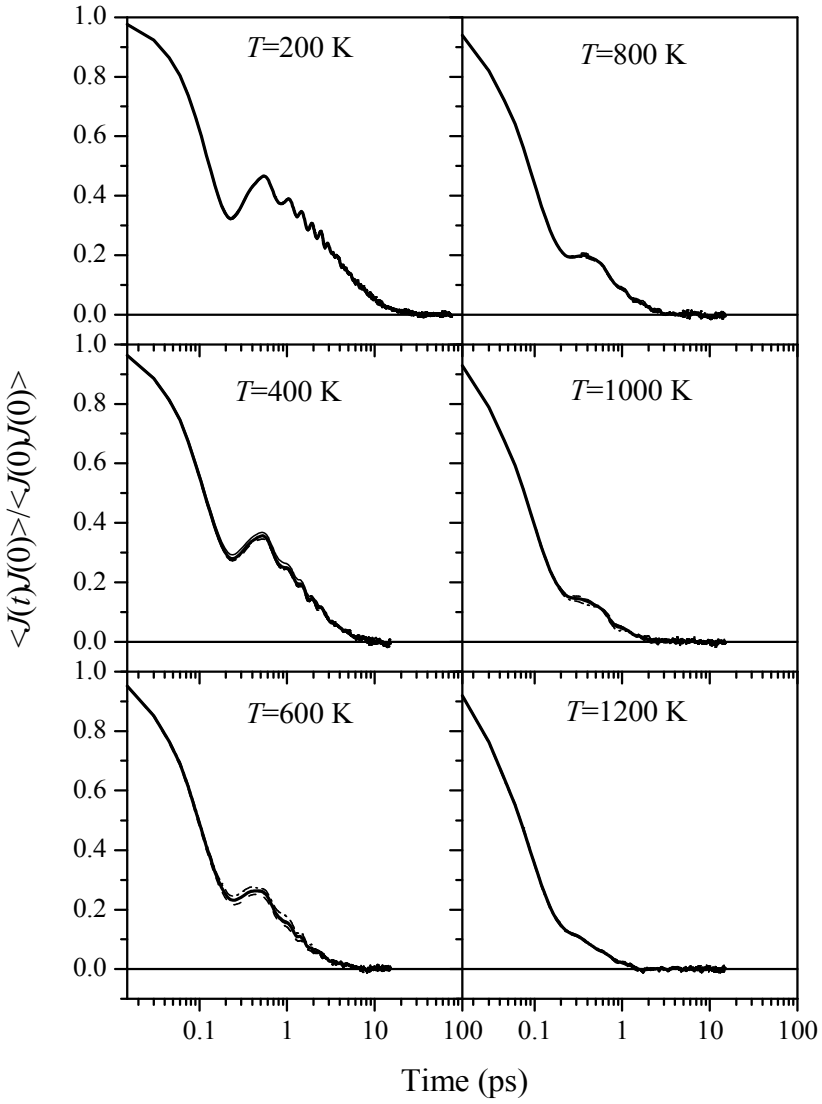

Fig. 2. Normalized heat current autocorrelation function at different temperatures for the *NPT* (thin solid line), *NVT* (dashed line) and *NVE* (dot-dashed line) ensembles as well as averaged over the three ensembles (thick solid line).

The temporal decay of the HCACF of the f.c.c. Cu model at low and intermediate temperatures demonstrates a more complex behaviour than the two-stage decay observed in [10,14] for the HCACF of the f.c.c. Ar model, which was described by two exponential functions (see Eq. (3)). Here, there is an initial rapid decay up to 0.2 – 0.25 ps. This stage is similar to the first stages of the HCACF decay of the f.c.c. Ar model observed in [10,14,15]. However, beyond this stage the HCACF of the f.c.c. Cu model show a peak around 0.5 ps in the temperature range 200 – 800 K. The intensity of the peak decreases as the temperature increases. At 900 K, it transforms to a plateau (shoulder) which diminishes almost entirely at 1200 K. Thus, only at very high temperatures, above 1200 K, the first stage decay of the HCACF of the f.c.c. Cu model is visually directly followed by a longer second stage decay and can be fitted by Eq. (3) (see Fig. 3), in accordance with the results reported in [10,14] for the HCACF of the f.c.c. Ar model for the whole studied temperature range. In the temperature range 900 – 1100 K, demonstrating a shoulder after the first decay, the HCACF of the f.c.c. Cu model is somewhat similar to the HCACF of the f.c.c. Ar model observed in [15] at low and intermediate temperatures. As we already mentioned the authors [15] associated this shoulder with collective oscillations of a transverse or shear nature. In the f.c.c. Cu model presented here, these oscillations have likely a much more pronounced character, so that the shoulder transforms to the peak in the HCACF of the model at lower and intermediate temperatures.

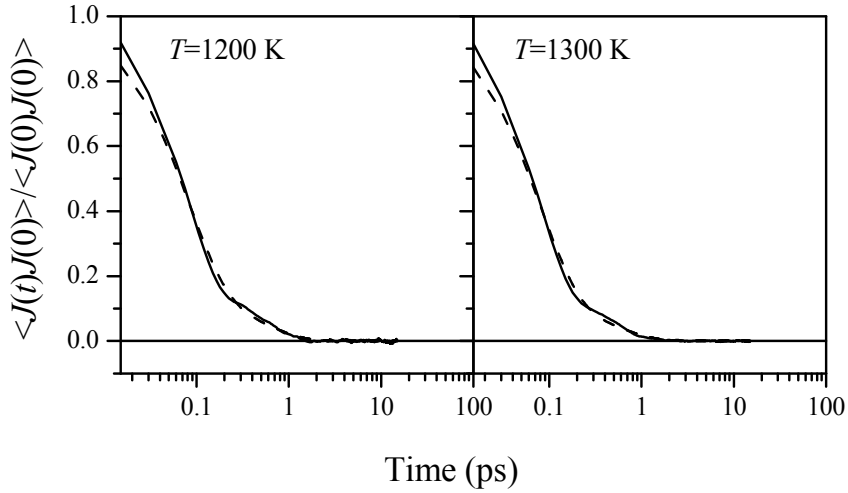

Fig. 3. Normalized heat current autocorrelation function averaged over *NPT*, *NVT* and *NVE* ensembles at 1200 and 1300 K (solid line) and its fit by the Eq. (3) (dashed line).

We suggest that the peak found in the f.c.c. Cu model (which does not appear in the f.c.c. Ar model [10,14,15]) may be activated by the influence of the positive (non-zero) Cauchy pressure C_{12}-C_{44} ≈50 GPa in f.c.c. Cu [23] on the phonon dynamics. Taking into account, the observed shape of the HCACF of the f.c.c. Cu model and three possible contributions to the lattice dynamics discussed above, we found that the HCACF of the f.c.c. Cu model can be nicely fitted by the following function:

$$\frac{1}{3}\langle \boldsymbol{J}(t)\boldsymbol{J}(0)\rangle = A\exp(-t/\tau)\cos\omega t + A_{\mathrm{ac,lg}}\exp\left(-t/\tau_{\mathrm{ac,lg}}\right). \quad (6)$$

Here, τ and A are the time constant and strength of the first-stage relaxation of the HCACF. It is recalled that in the literature there are two possible interpretations of the physical origin of this stage. According to McGaugey and Kaviany [10,14] this stage is associated with short wavelength acoustic phonons, while Kaburaki *et al.* [15] attribute it to single-particle motions sampling the local environment of the system. The contribution from the collective oscillations of a transverse or shear nature, as suggested in [15], we model in Eq. (6) by $\cos\omega t$, where ω can be described as a characteristic angular frequency of these oscillations. Lastly, $\tau_{\mathrm{ac,lg}}$ and $A_{\mathrm{ac,lg}}$ have the same meaning as in Eq. (3), namely, time constant and strength of the HCACF decay associated with long wavelength acoustic phonons.

The decomposition model, introduced here by Eq. (6), can capture all contributions discussed in the literature to the HCACF of a monatomic f.c.c. lattice. In particular, as can be seen in Fig. 4, it fits very well at all temperatures the HCACF of the f.c.c. Cu model. We also believe that Eq. (6) would properly fit the HCACFs of the f.c.c. Ar models calculated in [10,14,15]. Specifically, the more general decomposition model given by Eq. (6) in contrast to Eq. (3), would be able to describe the shoulder in the HCACF observed at short times in [15] at low and intermediate temperatures.

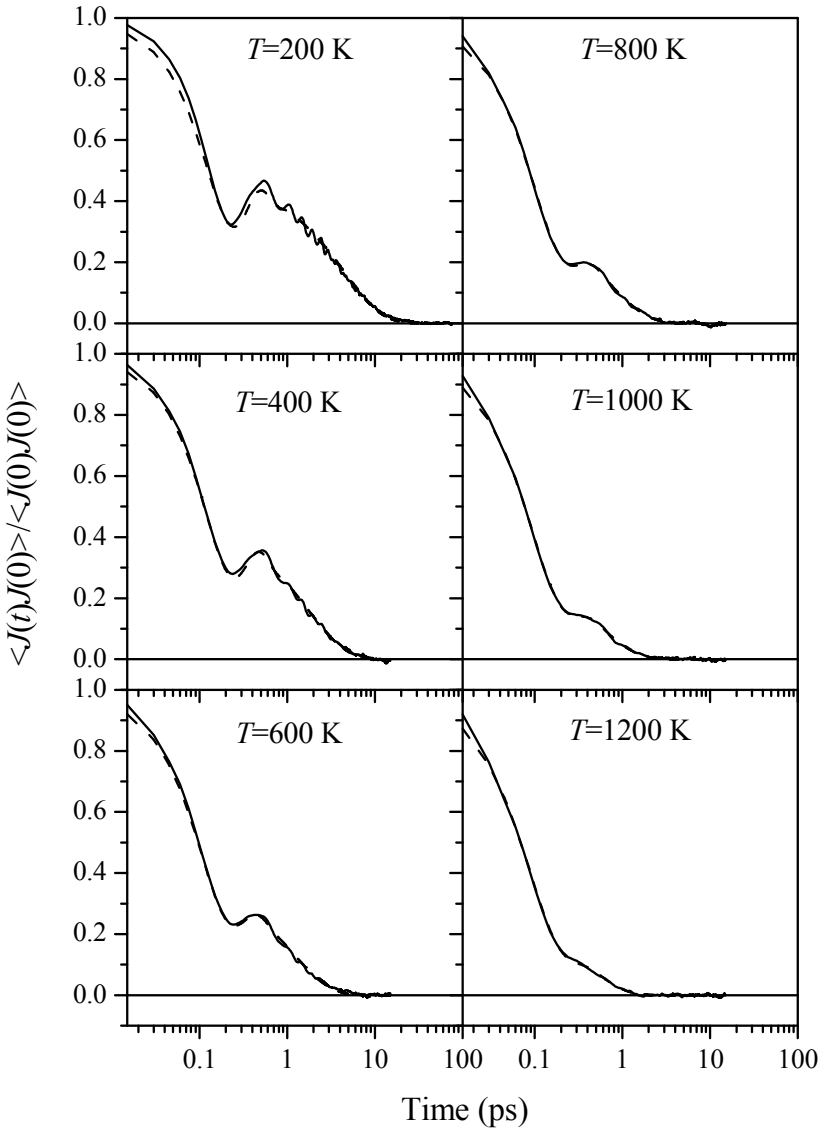

Fig. 4. Normalized heat current autocorrelation function averaged over *NPT*, *NVT* and *NVE* ensembles at 200, 400, 600,800, 1000 and 1200 K (solid line) and its fit by the Eq. (6) (dashed line).

In Figs. 5-7, we show the temperature dependence of the parameters of the decomposition model given by Eq. (6). It can be seen in Figs. 5 and 6 that for the f.c.c. Cu model, the temperature dependences of both strengths A and $A_{\mathrm{ac,lg}}$ as well as the temperature dependence of the time constant, $\tau_{\mathrm{ac,lg}}$, of the second stage of relaxation can be well fitted by the linear function in the double-logarithmic scale. As a result, the temperature dependencies of A, $A_{\mathrm{ac,lg}}$ and $\tau_{\mathrm{ac,lg}}$ can be approximated by the following equations:

$$A = A_{\mathrm{D}}\left(\frac{T}{T_{\mathrm{D}}}\right)^{n_A},\ A_{\mathrm{ac,lg}} = A_{\mathrm{D(ac,lg)}}\left(\frac{T}{T_{\mathrm{D}}}\right)^{n_{A(\mathrm{ac,lg})}},\ \tau_{\mathrm{ac,lg}} = \tau_{\mathrm{D(ac,lg)}}\left(\frac{T}{T_{\mathrm{D}}}\right)^{n_{\tau(\mathrm{ac,lg})}}, \qquad (7)$$

where the numerical values of the fitting parameters of both strengths (A_{D}, n_A and $A_{\mathrm{D(ac,lg)}}$, $n_{A(\mathrm{ac,lg})}$) and the time constant of the second stage of decay ($\tau_{\mathrm{D(ac,lg)}}$, $n_{\tau(\mathrm{ac,lg})}$) are listed in Table 1, T_{D}=343 K is the Debye temperature of Cu [25]. The use of T_{D} in Eq. (7) gives us a clear physical meaning for A_{D}, $A_{\mathrm{D(ac,lg)}}$ and $\tau_{\mathrm{D(ac,lg)}}$, namely, they represent the strengths and the time constant of the second stage of decay at the Debye temperature, respectively.

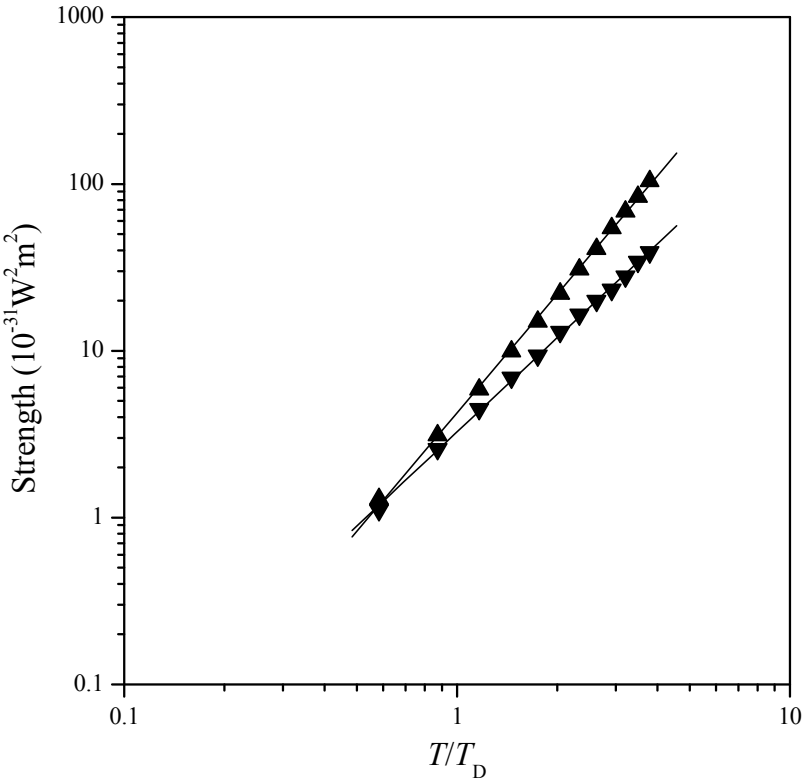

Fig. 5. Double-logarithmic plot of the temperature dependence of the strengths A (upward facing triangles) and $A_{\mathrm{ac,lg}}$ (downward facing triangles) calculated within the framework of HCACF decomposition given by Eq. 6 as applied to the f.c.c. Cu model. The solid lines show the linear fits of the data. T_{D}=343 K is the Debye temperature of Cu [25].

As can be seen in Fig. 6, the time constant of the first stage of decay, τ, shows a weak temperature dependence, decreasing from 0.176 ps at 200 K to 0.085 ps at 1300 K. If we assume that the energy transfer between neighbouring atoms occurs over one half of the period of oscillation of an atom [10,14,22,26] then the associated time constant can be estimated from the Debye temperature, T_{D}, as:

$$\tau_{\mathrm{D}} = \frac{2\pi}{2\omega_{\mathrm{D}}} = \frac{\pi\hbar}{k_{\mathrm{B}}T_{\mathrm{D}}}, \tag{8}$$

where ω_{D} is the Debye frequency and $\hbar$ is the Plank constant divided by 2π. The factor of two in the dominator is included as one half of oscillation is considered. Hence, the time constant for the energy transfer between neighbouring atoms in f.c.c. Cu can be estimated as τ_{D}=0.07 ps ($\omega_{\mathrm{D}} = k_{\mathrm{B}}T_{\mathrm{D}}/\hbar$ =44.906 THz). The comparison of these two constants shows that the calculated values of τ correspond to a few τ_{D} for the whole studied temperature range. Thus, the first time scale in the HCACF decomposition can be associated with the phonons that are in the high frequency range of the acoustic branches. These phonons have wavelengths on the order of a few atomic distances and may be referred as the short wavelength acoustic phonons [10,14].

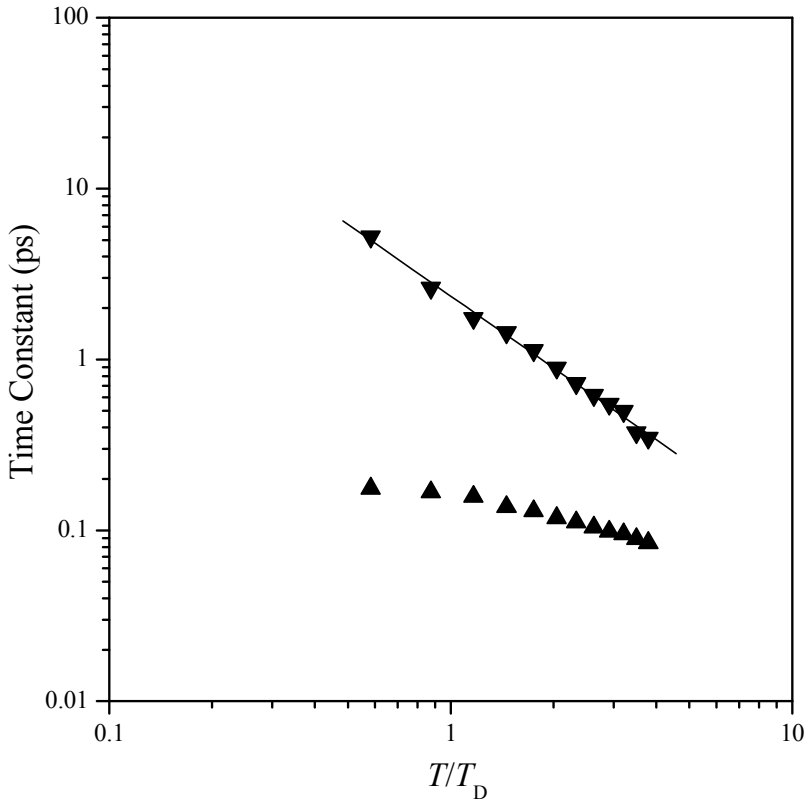

Fig. 6. Double-logarithmic plot of the temperature dependence of the time constants τ (upward facing triangles) and $\tau_{ac,lg}$ (downward facing triangles) calculated within the framework of HCACF decomposition given by Eq. 6 as applied to the f.c.c. Cu model. The solid line shows the linear fit of the data for $\tau_{ac,lg}$. T_D=343 K is the Debye temperature of Cu [25].

The second time scale in the HCACF decomposition can be associated with the phonons having an average characteristic angular frequency ω (see Eq. 6). Perhaps these oscillations may have transverse or shear nature as was suggested in [15]. As can be seen in Fig. 7, the characteristic frequency of these oscillations ω slightly decreases with temperature and is about four-five times lower than the Debye frequency. Thus, these phonons are in the medium frequency range of the acoustic branches.

The third time scale in the HCACF decomposition is associated with the long wavelength acoustic phonons. As can be seen in Fig. 6, the time constant of this stage of decay, $\tau_{ac,lg}$, shows a much stronger temperature dependence (see, also, Eq. (7) and Table 1) than the time constant of the first stage of decay, τ, decreasing from 5.23 ps at 200 K to 0.347 ps at 1300 K. This time constant is much more sensitive to temperature variations because long-range ordering is needed to sustain the collective motions in the low frequency range of the acoustic branches.

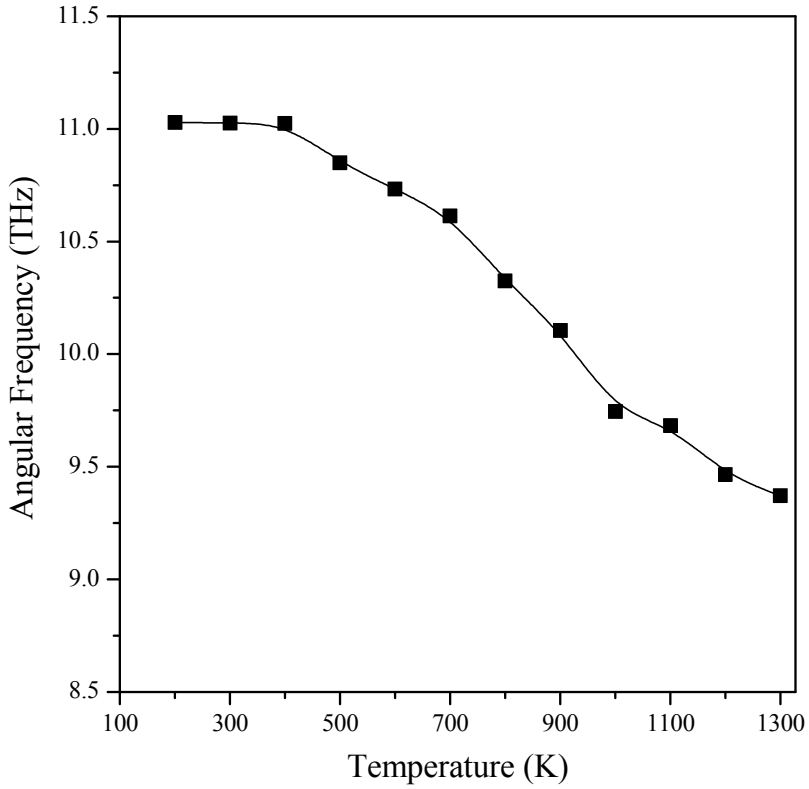

Fig. 7. Temperature dependence of the characteristic angular frequency calculated within the framework of HCACF decomposition given by Eq. 6 as applied to the f.c.c. Cu model. The solid curve is drawn by using a cubic B-spline fit of the data and is shown as a visual guide.

Table 1. Numerical values of the fitting parameters in Eq. (6), for the temperature dependencies of strengths A and $A_{\mathrm{ac,lg}}$ and the time constant of the second stage of decay $\tau_{\mathrm{ac,lg}}$, calculated for the f.c.c. Cu model within framework of the HCACF decomposition described by Eq. (5).

A		$A_{\mathrm{ac,lg}}$		$\tau_{\mathrm{ac,lg}}$	
A_{D} ($\mathrm{W^2m^2}$)	n_A	$A_{\mathrm{D(ac,lg)}}$ ($\mathrm{W^2m^2}$)	$n_{A\mathrm{(ac,lg)}}$	$\tau_{\mathrm{D(ac,lg)}}$ (ps)	$n_{\tau\mathrm{(ac,lg)}}$
4.25×10^{-31}	2.36	3.26×10^{-31}	1.87	2.35	-1.395

The temperature dependence of the phonon thermal conductivity, k, of the f.c.c. Cu model is shown in Fig. 8. We found that the temperature dependence of the phonon thermal conductivity of the f.c.c. Cu model can be well fitted by the linear function in the double-logarithmic scale (see Fig. 8). As a result, the temperature dependence of k can be approximated by the following equation:

$$k = k_{\mathrm{D}} \left(\frac{T}{T_{\mathrm{D}}}\right)^{n_k}, \tag{9}$$

where k_{D} ≈10.06 W/mK is the thermal conductivity at the Debye temperature T_{D} and n_k ≈-1.41. We can see that the numerical value found of the exponent demonstrates that the temperature dependence of the thermal conductivity of the f.c.c. Cu model varies more rapidly than T^{-1} which is predicted by the theory [25,27]. However, our results are in good agreement with the calculations [15] on the f.c.c. Ar model which predict the exponent value of about -1.35. In addition, we can point out that the calculated thermal conductivity of the f.c.c. Cu model is about one order of magnitude higher than that of the f.c.c. Ar model [10,14,15]. We believe that a larger value of phonon thermal conductivity predicted by an EAM potential model compared to a pair potential model can be explained by the inclusion of the electronic contribution to the bulk lattice properties during the fitting of the EAM potential functions to the experimental or *ab initio* data. Also, our

data on the thermal conductivity are in agreement with the abovementioned calculations of the phonon thermal conductivity of f.c.c Cu under a large temperature gradient (using heat baths at 300 and 850 K at the ends of the simulation cell) [6] with an older EAM potential [8]. In particular, the numerical value of the thermal conductivity found in [6], 5.7 W/mK (which probably should be related to the temperature 575 K at the the middle of the simulation cell), is between the thermal conductivities 6.54 and 4.85 W/mK calculated in the present work at 500 and 600 K, respectively.

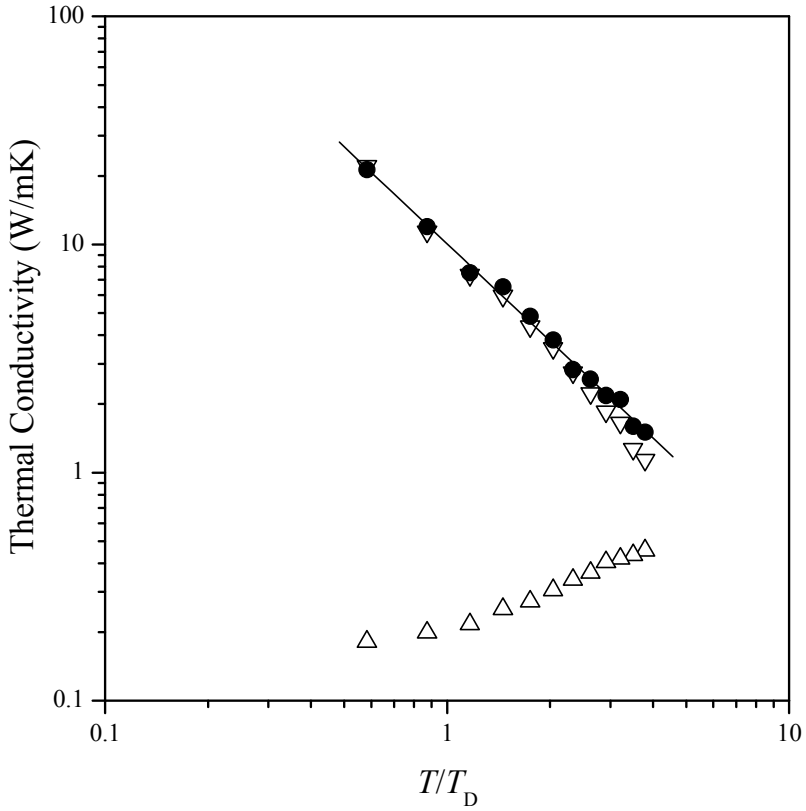

Fig. 8. Double-logarithmic plot of the temperature dependence of the thermal conductivity of the f.c.c. Cu model. The solid line shows the linear fit of the data. Upward facing triangles ($k_{\tau\omega}$) and downward facing triangles ($k_{\mathrm{ac,lg}}$) show the decomposition of the thermal conductivity given by Eq. (10). The T_{D}=343 K is the Debye temperature of Cu [25].

Substituting the introduced HCACF decomposition model, given by Eq. (6), into Eq. (1) the thermal conductivity can be represented as:

$$k = \frac{1}{Vk_{\mathrm{B}}T^2}\left(A\frac{\tau}{1+\tau^2\omega^2} + A_{\mathrm{ac,lg}}\tau_{\mathrm{ac,lg}}\right) = k_{\tau\omega} + k_{\mathrm{ac,lg}}, \qquad (10)$$

where $k_{\tau\omega}$ is the part of the thermal conductivity which takes into account those phonons that are in the high and medium frequency range of the acoustic branches, while phonons with lower frequencies (longer mean free paths) are accounted for by the second term $k_{\mathrm{ac,lg}}$. Extracted from Eq. (10) the temperature dependencies of these two parts of the thermal conductivity of the f.c.c. Cu model are also shown in Fig. 8. The second term in Eq. (10) has a similar meaning as the second term in Eq. (4), and contains most of the temperature dependence of the thermal conductivity (see Fig. 8). For instance, its relative contributions to the thermal conductivity are about 0.99 and 0.7 at 200 and 1300 K, respectively.

In additional studies we have not observed either an effect of size of the simulation cell or an effect of the length of the production run on the HCACF. In particular, Fig. 9 gives the comparison of the HCACFs of the f.c.c. Cu model at 500 K predicted from the simulation blocks

containing 4,000 and 32,000 atoms, using production runs of $10^7\Delta t$ and $2\times10^6\Delta t$, respectively; while Fig. 10 shows the comparison of the HCACF calculations performed with the simulation block composed of 4,000 atoms at the temperatures 500, 700 and 1300 K, using production runs of $10^6\Delta t$ and $10^7\Delta t$. As can be seen in Figs. 9 and 10, in all cases good agreement between the calculations can be observed. This comparison is additional confirmation of the reliability of our results.

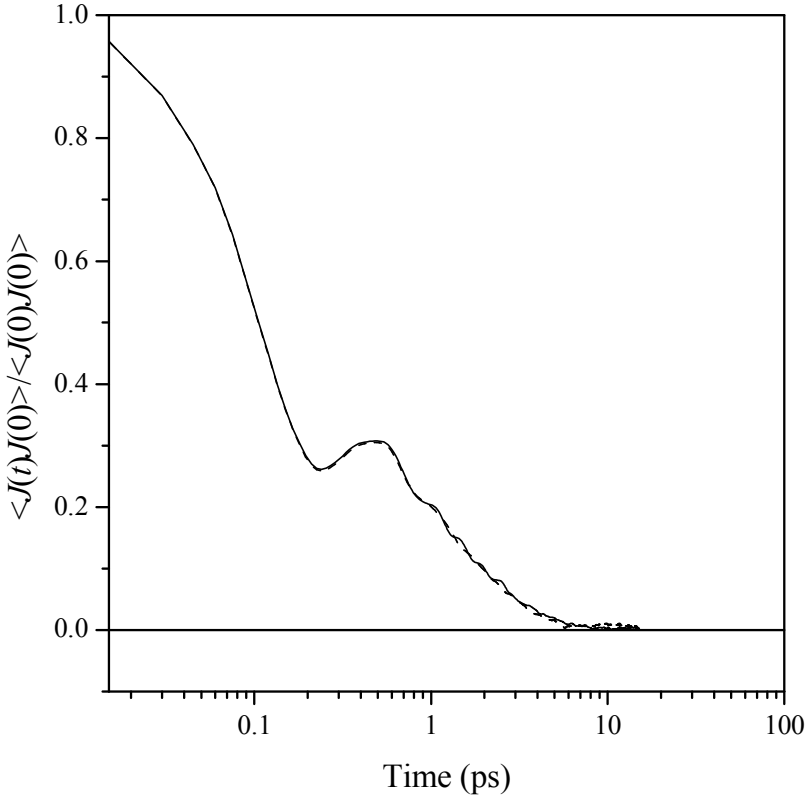

Fig. 9. Comparison of the normalized heat current autocorrelation functions of the f.c.c. Cu model calculated with the simulation blocks containing 4,000 (solid line) and 32,000 (dashed line) atoms, using production runs of $10^7\Delta t$ and $2\times10^6\Delta t$, respectively.

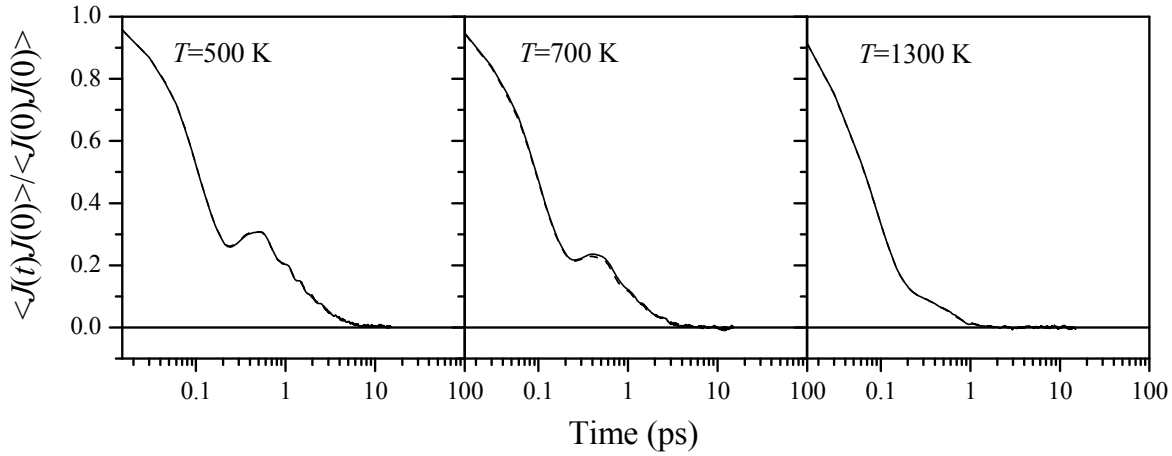

Fig. 10. Comparison of the normalized heat current autocorrelation functions of the f.c.c. Cu model calculated with the simulation block composed of 4,000 atoms at temperatures 500, 700 and 1300 K, using production runs of $10^6\Delta t$ (solid line) and $10^7\Delta t$ (dashed line).

Finally, in Fig. 11, we compare our results on the phonon thermal conductivity of f.c.c. Cu model with experimental measurements of the thermal conductivity [28], which include also the electronic contribution. It can be seen in Fig. 11 that the electronic contribution to the total thermal conductivity of f.c.c. Cu dominates over the whole studied temperature range. Nevertheless, the phonon contribution to the total thermal conductivity of f.c.c. Cu increases as temperature decreases. It can be estimated as about 0.5 % at 1300 K and about 5 % at 200 K (see Fig. 11(b)).

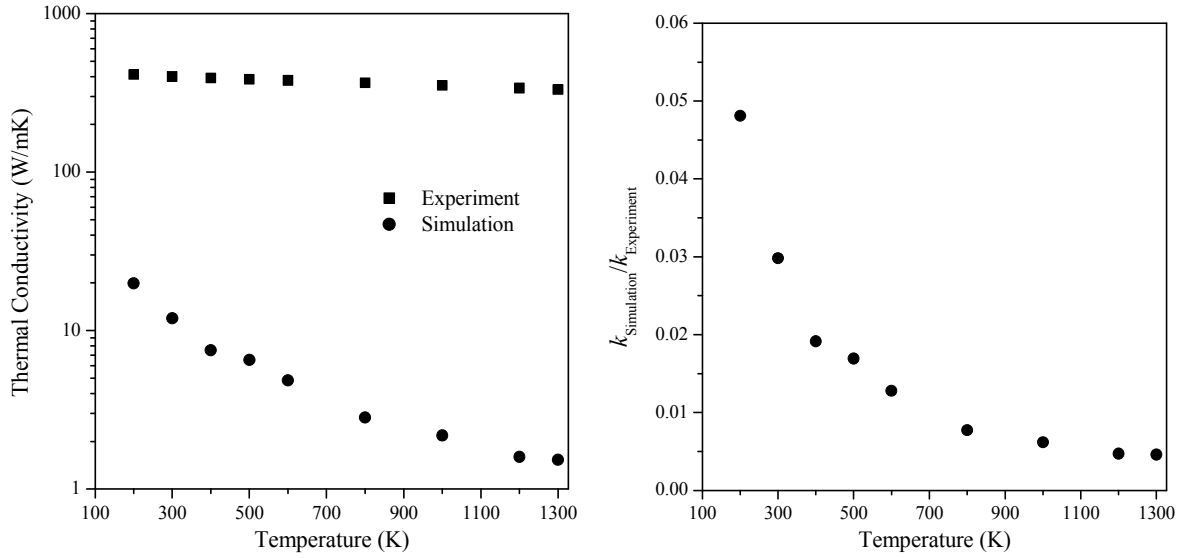

(a) (b)

Fig. 11. (a) Comparison of the temperature dependences of the calculated phonon thermal conductivity of the f.c.c. Cu model with experimental measurements of the thermal conductivity [28], which include also the electronic contribution. (b) Temperature dependence of the ratio between the simulation data and experimental measurements [28] on the thermal conductivity of f.c.c. Cu.

Conclusions

Phonon dynamics and phonon thermal conductivity of f.c.c. Cu have been investigated in detail in the temperature range 200 – 1300 K within the framework of the equilibrium MD simulations in conjunction with the GK formalism, using one of the most reliable EAM potentials [23].

It has been found that the temporal decay of the HCACF of the f.c.c. Cu model at low and intermediate temperatures demonstrate a more complex behaviour than the two-stage decay observed previously in the HCACF of the f.c.c. Ar model, [10,14,15]. Namely, an initial rapid decay of the HCACF of the f.c.c. Cu model up to 0.2 – 0.25 ps followed by a peak around 0.5 ps in the temperature range 200 – 800 K. The intensity of the peak decreases as the temperature increases. At 900 K, it transforms to a shoulder which diminishes almost entirely at 1200 K. Thus, only at very high temperatures, above 1200 K, the first stage decay of the HCACF of the f.c.c. Cu model is visually directly followed by a longer second stage decay in accordance with the results reported in [10,14] for the HCACF of the f.c.c. Ar model. In the temperature range 900 – 1100 K, demonstrating a shoulder after the first decay, the HCACF of the f.c.c. Cu model is somewhat similar to the HCACF of the f.c.c. Ar model observed in [15] at low and intermediate temperatures. The authors [15] associated this shoulder with collective oscillations of a transverse or shear nature. In the f.c.c. Cu model, these oscillations have likely to have a much more pronounced character, so that the shoulder transforms to the peak in the HCACF of the model at lower and intermediate temperatures.

We have suggested that the peak found in the f.c.c. Cu model (which does not appear in the f.c.c. Ar model [10,14,15]) may be activated by the influence of the positive (non-zero) Cauchy pressure C_{12}-C_{44} ≈50 GPa in f.c.c. Cu [23] on the phonon dynamics.

We have introduced the HCACF decomposition model (see Eq. (6)), that can capture all contributions discussed in the literature to the HCACF of a monatomic f.c.c. lattice. In particular, this HCACF decomposition model allows us to distinguish three time scales in the phonon dynamics. The first time scale in the HCACF decomposition can be associated with phonons that are in the high frequency range of the acoustic branches. These phonons have wavelengths of the order of a few atomic distances and may be referred as short wavelength acoustic phonons [10,14]. The second time scale in the HCACF decomposition can be associated with phonons having an average characteristic angular frequency about four-five times lower than the Debye frequency. These phonons are in the medium frequency range of the acoustic branches and possibly may have a transverse or shear nature, as was suggested in [15]. The third time scale in the HCACF decomposition is associated with the long wavelength acoustic phonons which are responsible for most of the temperature dependence of the thermal conductivity. The dynamics of these phonons is much more sensitive to temperature variations because long-range ordering is needed to sustain the collective motions in the low frequency range of the acoustic branches.

We have found that the temperature dependence of the phonon thermal conductivity of the f.c.c. Cu model can be well fitted to a linear function in a double-logarithmic scale, giving an exponent of about -1.41. The numerical value found of the exponent demonstrates that the temperature dependence of the thermal conductivity of the f.c.c. Cu model varies more rapidly than T^{-1} which is predicted by the theory [25,27]. However, our results are in good agreement with the calculations [15] on the f.c.c. Ar model which predict an exponent value of about -1.35.

We have demonstrated that the calculated thermal conductivity of the f.c.c. Cu model is about one order of magnitude higher that of the f.c.c. Ar model [10,14,15]. We believe that a larger value of phonon thermal conductivity predicted by an EAM potential model compared to a pair potential model can be explained by the including of the electronic contribution to the bulk lattice properties during the fitting of the EAM potential functions to the experimental or *ab initio* data.

We have shown that within the framework of the introduced HCACF decomposition model, the thermal conductivity can be represented as a sum of two contributions. The first part of the thermal conductivity takes into account those phonons that are in the high and medium frequency range of the acoustic branches, while phonons with lower frequencies (longer mean free paths) are accounted for by the second term. The second term contains the most of the temperature dependence of the thermal conductivity.

By comparison of our results on the phonon thermal conductivity of f.c.c. Cu model with experimental measurements of the thermal conductivity [28], which include also the electronic contribution, we have shown that the electronic contribution to the total thermal conductivity of f.c.c. Cu dominates over the whole studied temperature range. Nevertheless, the phonon contribution to the total thermal conductivity of f.c.c. Cu increases as the temperature decreases. The contribution can be estimated at about 0.5 % at 1300 K and about 5 % at 200 K.

Acknowledgements

This research was supported by the Australian Research Council through its Discovery Project Grants Scheme.

References

[1] Y. Mishin, M. Asta and J. Li, *Acta Mater.*, 2010, 58, 1117.

[2] M.E. Glicksman and R.J. Schaefer, *J. Cryst. Growth*, 1988, 1, 297.

[3] G.H. Rodway, J.D. *Hunt*, *J. Cryst. Growth*, 1991, 112, 554.

[4] J.J. Hoyt, M. Asta, A. Karma, *Interface Sci.*, 2002, 10, 181.

[5] J. Monk Y. Yang, M.I. Mendelev *et al.*, *Modelling. Simul. Mater. Sci. Eng.*, 2010, 18, 015004.

[6] C.F. Richardson, P. Clancy, *Phys. Rev.*, 1992, B 45, 12260.

[7] M. Daw and M.I. Baskes, *Phys. Rev.*, 1984, B 29, 6443.

[8] S.M. Foiles, M.I. Baskes and M.S. Daw, *Phys. Rev.*, 1986, B 33, 7983.

[9] W. Ashcroft and N.D. Mermin, *Solid State Physics* (Saunders College, Philadelphia, 1976).

[10] A.J.H. McGaughey and M. Kaviany, *Advances in Heat Transfer*, 2006, 39, 169.

[11] M.S. Green, *J. Chem. Phys.*, 1954, 22, 398.

[12] R. Kubo, *J. Phys. Soc. Japan*, 1957, 12, 570.

[13] D.A. McQuarrie, *Statistical Mechanics* (Harper & Row, New York, 1967).

[14] A.J.H. McGaughey and M. Kaviany, *International Journal of Heat and Mass Transfer*, 2004, 47, 1783.

[15] H. Kaburaki, J. Li, S. Yip and H. Kimizuka, *Journal of Applied Physics*, 2007, 102, 043514.

[16] I.N. Krupskii and V.G. Manzhelii, *Sov. PPhys. JETP*, 1969, 28, 1097.

[17] D.K. Christen and G.L. Pollack, *Phys. Rev.*, 1975, B 12, 3380.

[18] R.E. Peierls, *Ann. Phys.*, 1929, 3, 1055.

[19] A.J.C. Ladd, B. Moran and W.G. Hoover, *Phys. Rev.*, 1986, B 34, 5058.

[20] J. Che, T. Cagin, W. Deng and W.A. Goddard III, *J. Chem. Phys.*, 2000, 113, 6888.

[21] D.G. Cahill and R.O. Pohl, *Solid State Commun.* 1989, 70, 927.

[22] D.G. Cahill, S.K. Watson and R.O. Pohl, *Phys. Rev.*, 1992, B 46, 6131.

[23] Y. Mishin, M.J. Mehl, D.A. Papaconstantopoulos, A.F. Voter and J.D. Kress, *Phys. Rev.*, 2001, B 63, 224106.

[24] *Binary Alloy Phase Diagrams*, edited by T.B. Massalski (ASM, Materials Park, OH, 1986).

[25] C. Kittel, *Introduction to Solid State Physics* (Wiley, New York, 1971).

[26] A. Einstein, *Ann. Phys.*, 1911, 35, 679.

[27] J.M. Ziman, *Electrons and Phonons: The Theory of Transport Phenomena in Solids* (Clarendon Press, Oxford, 1960).

[28] C.Y. Ho, R.W. Powell and P.E. Liley, *J. Phys. Chem. Ref. Data*, 1972, 1, 279.

Heat Transfer Processes in Engineering Materials
10.4028/www.scientific.net/DDF.336

Phonon Thermal Conductivity of F.C.C. Cu by Molecular Dynamics Simulation
10.4028/www.scientific.net/DDF.336.169